Angular momentum kinetics in intersubband transitions in semiconductor quantum wells

Robert J. Steed, Mark D. Frogley, Mary Matthews, Edmund Clarke, Ray Murray, and Chris C. Phillips
Department of Physics, Experimental Solid State Group, Imperial College London, London SW7 2AZ, United Kingdom

H. Luo and H. C. Liu
Institute for Microstructural Sciences, National Research Centre, Ottawa, Canada K1A 0R6
(Received 23 May 2008; revised manuscript received 28 July 2008; published 19 November 2008)

A bonded rhomb sample geometry is used to study the spin-dependent absorption characteristics of an intersubband transition in the conduction band of a GaAs/AlGaAs quantum well. Optical saturation experiments, using linearly and circularly polarized beams, were compared to measure the population relaxation time of the upper subband and the degree to which spin polarization is occurring in the electron population. In sharp contrast to previous interband absorption studies, the intersubband data are consistent with a picture in which the angular momentum of the incident photons appears to bypass the electron system completely and instead exerts a direct torque on the crystal lattice.

DOI: 10.1103/PhysRevB.78.205319 PACS number(s): 78.66.Fd

I. INTRODUCTION

The ability to optically orientate the electron spins in semiconductor systems is of interest both as a means of studying spin relaxation and precession kinetics and because of the potential for accessing the electron-spin quantum number for spintronic device applications.[1] To date, optical spin orientation studies have typically employed interband excitation, and in the case of semiconductor quantum wells (QWs), since the valence-band spin degeneracy is lifted by confinement, close to 100% spin polarization can be achieved.[1]

In comparison, spin orientation based on absorption by QW intersubband transitions (ISBTs) offers the advantage of involving only one type of carrier; this avoids the creation of excitons and removes the large hole scattering contribution to spin relaxation due to the Bir-Aronov-Pikus mechanism.[1] The conduction-band states in GaAs QWs derive from $J=1/2$ atomic orbitals and a photon carries a single unit of angular momentum (aligned parallel or antiparallel to the light propagation direction). This implies that a direct optical-absorption process, which links two conduction-band electron states, will flip the sign of the electron-spin component along this axis. Indeed, spin-sensitive experiments involving ISBTs have been previously observed with obliquely incident light in *n*-type QW samples[2] and at normal incidence in *p*-type QWs.[3] In both cases a highly sensitive background-free photocurrent method was used to detect the spin polarization of the carrier populations following ISBT absorption of circularly polarized light.

The present studies were driven by the prospect of being able to manipulate and detect the spins of electrons in solid-state systems by all-optical means. We study the way the electron system absorbs and dissipates the angular momentum contained in a beam of circularly polarized photons by measuring the optical saturation properties of a resonantly excited electron ISBT in a GaAs/AlGaAs multiple QW (MQW) sample. In principle, using circularly polarized infrared (IR) radiation to excite spin-sensitive transitions can lead to a spin-polarized carrier population through a "spin-pumping" effect.[4] This will happen in a way that is similar to that previously seen with heavy-hole 1 to light-hole 1 transitions in AlGaAs/GaAs QWs,[5] but the situation will be considerably simplified by the straightforward $J=1/2$ character of the conduction-band spin system.

In the classical view of optical absorption, the two-dimensional (2D) nature of the electrons in a QW means absorption by ISBTs is characterized by an optical dipole which is polarized normal to the QW plane.[6] ISBT spectroscopic measurements typically exploit this extreme dichroism to ratio out substrate absorption artifacts by using orthogonally polarized beam measurements, usually in a rhomb-shaped sample. It also has the practical consequence that ISBT based *n*-type detectors absorb normally incident radiation only very weakly and need carefully designed radiation coupling schemes to work efficiently.[7]

For these experiments we developed a rhomb-shaped bonded wafer structure which enabled us to compare the saturation characteristics of the ISBT in a AlGaAs/GaAs QW with intense linearly and circularly polarized IR light pulses in order to compare their saturation intensities and look for evidence of spin pumping. IR light was generated as a single frequency, well collimated, tunable beam from a laser-based Optical Parametric Generator. This allowed intense circularly polarized beams to be produced to resonantly excite ISBTs in the technologically challenging mid-IR part of the spectrum.

In the following, Sec. II A describes how the basic theory of optical saturation can be adapted to apply to the present spin-dependent experiments and Sec. II B covers the theory of saturable spin pumping. In Sec. III, we describe the QW sample and the experiments carried out. The results are presented in Sec. IV. Section V is a brief conclusion.

II. THEORY

A. Saturation of intersubband transitions

In an optical saturation experiment, the fraction of incident light absorbed by a sample drops at high intensities.[8] This occurs because the number of electrons in the sample is finite, and each takes a finite spontaneous relaxation time, τ_{21}, to return to its ground state before it can absorb another

photon. In contrast to the atomic case (where the spontaneous relaxation rate is determined by photon emission and is readily calculable), in solid-state systems this spontaneous relaxation time involves a myriad of types of electron-lattice interaction.[9]

In the case of an ISBT this relaxation time is typically ~1 ps; so a significant redistribution of electrons between the energy levels occurs only when, at high laser intensities, the excitation rate per electron approaches $(1\ \text{ps})^{-1}$. This process can be well described using a standard rate equation model.[8] The number of electrons in the system is fixed so the rate of change in electron population in levels 1 must be equal and opposite to that of level 2, where

$$\frac{dN_1}{dt} = -\frac{dN_2}{dt} = (N_2 - N_1)\sigma\Phi + \frac{N_2}{\tau_{21}}, \tag{1}$$

where N_1 and N_2 are the population densities of the lower and upper levels, σ is the small-signal absorption cross section of the transition, Φ is the photon flux, and τ_{21} is the relaxation time. Taking N as the areal density of electrons, then solving Eq. (1) in the steady state gives

$$N_1 = \frac{1 + \tau_{21}\sigma\Phi}{1 + 2\tau_{21}\sigma\Phi}N, \tag{2}$$

$$N_2 = \frac{\tau_{21}\sigma\Phi}{1 + 2\tau_{21}\sigma\Phi}N. \tag{3}$$

The absorption of light through a sample can then be calculated using[8]

$$\frac{\partial I}{\partial z} = -(N_1 - N_2)\sigma I, \tag{4}$$

where $I = \hbar\omega_{12}\Phi$ is the intensity of the monochromatic light beam. This leads to

$$\frac{\partial I}{\partial z} = -\frac{\sigma N}{1 + I/I_{\text{sat}}}I, \tag{5}$$

where the saturation intensity parameter, I_{sat}, is given by

$$I_{\text{sat}} = \frac{\hbar\omega_{12}}{2\sigma\tau_{21}}. \tag{6}$$

In the case of ISBTs, adjustments must be made to account for the QW's 2D geometry and because the ISBT's absorption is anisotropic.[10] An effective absorption coefficient (with dimensions m^{-1}) for the MQW is defined via the effective electron density, $n_{\text{QW}}\,\sigma/d$, where d is the period of the MQW structure and n_{QW} is the 2D sheet electron density per QW. The dimensionless small-signal fractional absorption for the whole MQW structure is then given by

$$\alpha_{12} = n_{\text{QW}}\sigma M\frac{\sin^2\theta}{\cos\theta}, \tag{7}$$

where M is the number of QWs in the sample and θ is the angle between the radiation propagation direction and the QW normal.

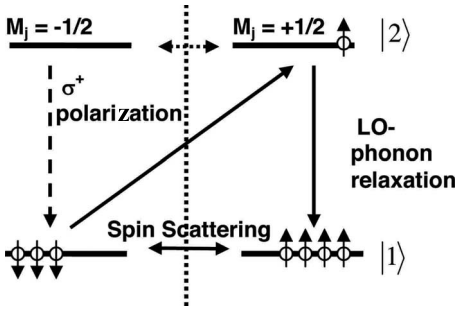

FIG. 1. Electron dynamics for the case of absorption of circularly polarized light flipping the spin of an electron during an ISBT absorption event. If the spin-relaxation time, τ_s, is long compared with the population relaxation time, τ_{21}, the spin-scattering step will result in a reduced saturation intensity compared to that seen in a linearly polarized light experiment, and at high intensities of light, a spin-pumped population of spin-up electrons will be created.

The saturation intensity is also affected by the anisotropic absorption of the ISBTs but this can be factored out using Eq. (7), leading to

$$I_{\text{sat}} = \frac{n_{\text{QW}}\hbar\omega_{12}M}{2\alpha_{12}\tau_{12}}. \tag{8}$$

Equation (8) can be used to extract a relaxation-time value from an experimentally measured saturation intensity parameter. In the case of ISBTs, the relaxation mechanism is dominated by nonradiative relaxation via LO phonon emission.[6]

In practice, I_{sat} values are so high that focused and pulsed beams have to be used so the excitation intensity varies temporally and spatially. In this case the fit to the experimental data has to be done by numerically integrating Eq. (5) (Ref. 8) in a way that accounts for the initial (in this case Gaussian in both space and time) intensity distribution and the way it decreases as it passes through the sample.[10]

The experiment uses a beam focused into the sample with a Rayleigh length of 1 mm, but once inside the ~500-μm-thick sample the GaAs refractive index increases this[11] to 3.3 mm so it in fact closely approximates the ideal of a perfectly collimated beam.

Finally, the interpretation of saturation data obtained from standard rhomb-shaped IBST samples can be complicated by the possibility of standing-wave effects due to the way the IR light is reflected at the sample-air interfaces.[10] However, the wafer bonded sample allows us to avoid this problem by using a traveling-wave geometry (Sec. III).

B. Spin pumping of intersubband transitions

The $J = 1/2$ conduction subbands of a GaAs QW can either be spin up or down with respect to the radiation propagation direction implying that a given handedness of circularly polarized light should only couple to electrons of a particular spin (Fig. 1).

The absorption saturation of such a system can be modeled with the following standard system of coupled rate equations:[4]

$$\frac{dN_{1\downarrow}}{dt} = (N_{2\uparrow} - N_{1\downarrow})\sigma'\Phi + \frac{N_{2\downarrow}}{\tau_{21}} + \frac{N_{1\uparrow} - N_{1\downarrow}}{\tau_s}, \tag{9a}$$

$$\frac{dN_{2\uparrow}}{dt} = (N_{1\downarrow} - N_{2\uparrow})\sigma'\Phi - \frac{N_{2\uparrow}}{\tau_{21}} + \frac{N_{2\downarrow} - N_{2\uparrow}}{\tau_s}, \tag{9b}$$

$$\frac{dN_{1\uparrow}}{dt} = \frac{N_{2\uparrow}}{\tau_{21}} + \frac{N_{1\downarrow} - N_{1\uparrow}}{\tau_s}, \tag{9c}$$

$$\frac{dN_{2\downarrow}}{dt} = -\frac{N_{2\downarrow}}{\tau_{21}} + \frac{N_{2\uparrow} - N_{2\downarrow}}{\tau_s}, \tag{9d}$$

$$N = N_{1\downarrow} + N_{1\uparrow} + N_{2\downarrow} + N_{2\uparrow}, \tag{9e}$$

where τ_s is the spin-relaxation time and σ' is the absorption cross section. It is assumed that population relaxation between the subbands occurs dominantly via the spin-conserving emission of LO phonons.

The steady-state solutions were found by rewriting Eqs. (9a)–(9e) in matrix form and using standard inversion techniques[12] to get

$$N_{1\downarrow} = \frac{(\tau_s + 2\tau_{21}) + \sigma'\Phi(\tau_s + \tau_{21})\tau_{21}}{2(\tau_s + 2\tau_{21}) + \sigma'\Phi(\tau_s + 2\tau_{21})^2}N, \tag{10a}$$

$$N_{2\uparrow} = \frac{\sigma'\Phi(\tau_s + \tau_{21})\tau_{21}}{2(\tau_s + 2\tau_{21}) + \sigma'\Phi(\tau_s + 2\tau_{21})^2}N, \tag{10b}$$

$$N_{1\uparrow} = \frac{(\tau_s + 2\tau_{21}) + \sigma'\Phi(\tau_s + \tau_{21})^2}{2(\tau_s + 2\tau_{21}) + \sigma'\Phi(\tau_s + 2\tau_{21})^2}N, \tag{10c}$$

$$N_{2\downarrow} = \frac{\sigma'\Phi\tau_{21}^2}{2(\tau_s + 2\tau_{21}) + \sigma'\Phi(\tau_s + 2\tau_{21})^2}N. \tag{10d}$$

The overall degree of spin polarization of the system is then given by

$$S \equiv (N_\uparrow - N_\downarrow)/N = \frac{\sigma'\Phi\tau_s}{2 + \sigma'\Phi(\tau_s + 2\tau_{21})}, \tag{11}$$

and it can be seen that the system becomes more spin polarized ($S \to 1$) *at higher* excitation intensities.

Under these assumptions, the saturation characteristics of this system when excited with circularly polarized light can be calculated using

$$\frac{\partial I}{\partial z} = -(N_{1\downarrow} - N_{2\uparrow})\sigma' I, \tag{12}$$

which leads to

$$\frac{\partial I}{\partial z} = -\frac{0.5\sigma' N}{1 + I/I'_{\text{sat}}}I, \tag{13}$$

where the fact that the low intensity absorption is half that of linearly polarized light reflects the fact that, at thermal equilibrium, only half the system's electrons can interact with the incoming beam. The saturation intensity is then given by

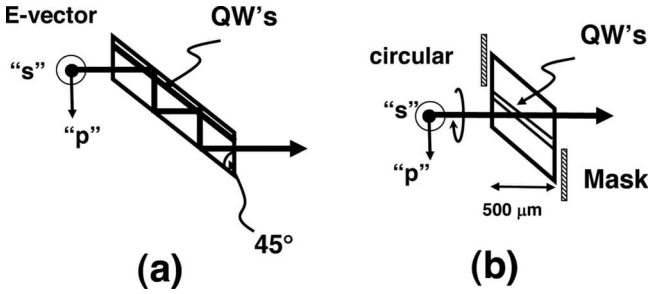

FIG. 2. Side views of two sample geometries that are used for optical experiments on ISBTs; the depth into the page of each were typically 5–10 mm. In the (a) rhomb geometry, light passes through the QWs multiple times due to the total internal reflections. The bonded (b) wafer sample geometry allows measurements to be made with circularly polarized beams without their polarization states being corrupted by the optical phase shifting that occurs when the light reflects from a oblique dielectric interface.

$$I'_{\text{sat}} = \frac{2\hbar\omega}{\sigma'(\tau_s + 2\tau_{21})}. \tag{14}$$

Interband excitation experiments have yielded literature values for the spin lifetimes, τ_s, typically ranging from 30 to 300 ps,[13,14] while typical population relaxation times, τ_{21}, are ~ 1 ps.[15] The above analysis (assuming that the absorption cross section, σ', is the same for spin-flipping transitions as for conventional transitions) implies that saturation intensities measured with linearly and circularly polarized light should differ by a factor of $(\tau_s + 2\tau_{21})/4\tau_{21}$, which evaluates to somewhere between ~ 10 and 80.

III. EXPERIMENTAL SETUP

The sample studied came from a molecular-beam epitaxy (MBE)-grown wafer that contained 50 QWs, each consisting of a 6.3-nm-thick GaAs layer, *n*-doped with silicon at 2×10^{18} cm^{-3}, and separated by 30-nm-wide $Al_{0.31}Ga_{0.69}As$ barriers. The multiple QW structure was grown on a 350-μm-thick insulating (100) GaAs substrate and capped with 145 nm of undoped GaAs.

The comparatively high ($n = 3.3$) GaAs refractive index means that in a typical rhomb-shaped absorption sample [Fig. 2(a)], the relative phases of *s*-polarized and *p*-polarized components get phase shifted by almost $\pi/2$ at each total internal reflection (much like in a Fresnel rhomb). Circularly polarized light switches between being $\sim 100\%$ circularly polarized to almost $\sim 100\%$ linearly polarized with each bounce through the sample and this, combined with the standing-wave effects,[6,10] makes it impossible to use this geometry with circularly polarized beams.

Instead, two pieces of the wafer were fused together face to face resulting in the absorbing QW layer being embedded in the middle of much thicker, transparent, and index matched layers of bulk GaAs substrate material. The bonding was achieved by etching 100-nm-deep and 6-μm-wide grooves, spaced 400 μm apart into the top surface of the wafer, and then thermocompression bonding two pieces together for 30 min at a pressure of 1.2 MPa and a temperature of 800 K.

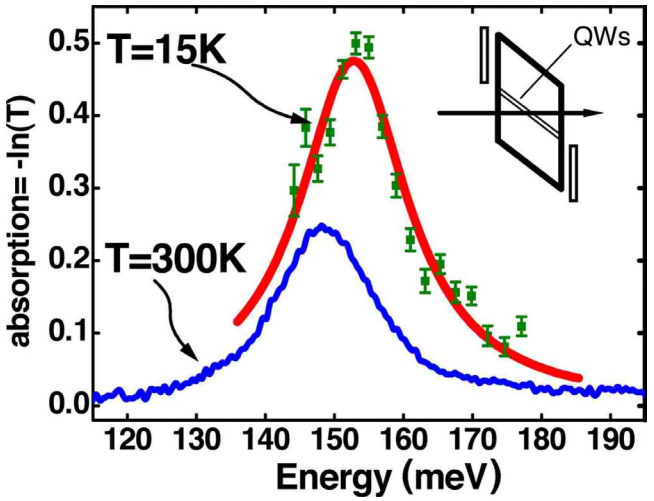

FIG. 3. (Color online) Low intensity ISBT absorption curves measured in the cryostat with the OPG laser (at $T=15$ K) and, separately, in a Fourier spectrometer at $T=300$ K. Both curves are plotted as ratios of the p to s linearly polarized spectra and the upper curve is a Lorentzian fit to the low-temperature data points which gave a linewidth of 19 (3) meV and transition wavelength [energy] of 8.1(1) μm [153(1) meV]. Inset: side view of the sample geometry showing the path of light through the quantum wells.

The resulting sandwich was then polished into a 500-μm-long rhomb geometry which was mounted and masked in such a way that light could enter and leave the sample at normal incidence so that its circular polarization state was unaffected as it entered the sample and passed straight through a total of 100 QWs at a 45° angle of incidence [Fig. 2(b)]. The polarization state of the detected light could now be directly and unambiguously related to the polarization state of the light interacting with the MQW layer.

Room-temperature (300 K) linearly polarized reference absorption spectra (Fig. 3) were taken using a standard Fourier spectrometer for comparison with low-temperature (15 K) spectra obtained with the sample in a closed-cycle cryostat and using the superior beam quality available from the laser-based optical parametric generator (OPG) source (see below). In both cases the transmitted s-polarized signal was used to correct for variations in the laser intensity (as the wavelength was tuned) and to ratio out spurious absorption features, in order to get absolute values for the ISBT absorption spectrum.

The saturation experiments were carried out using midinfrared light produced by parametric down conversion in a $ZnGeP_2$ crystal.[16] The idler beam from the crystal was tunable between the wavelengths $\lambda=6.4-8.6$ μm; each idler pulse contained ~9 μJ and was 100 ps long. The crystal was configured as an optical parametric generator[17] pumped by a mode-locked flashlamp-pumped Er^{3+}:Yttrium Scandium Gallium Garnet (YSGG) laser that produced 100 ps long pulses with a 2.8 μm wavelength at a repetition rate of 3 Hz. The infrared idler beam was focused to ~100 μm diameter beam spot on the bonded sample facet and peak intensities reached 200 MW cm^{-2}. The intensity distribution in the region of this focus was mapped out with a series of calibrated knife-edge tests and the pulse energy was measured using a calibrated large area pyroelectric detector.

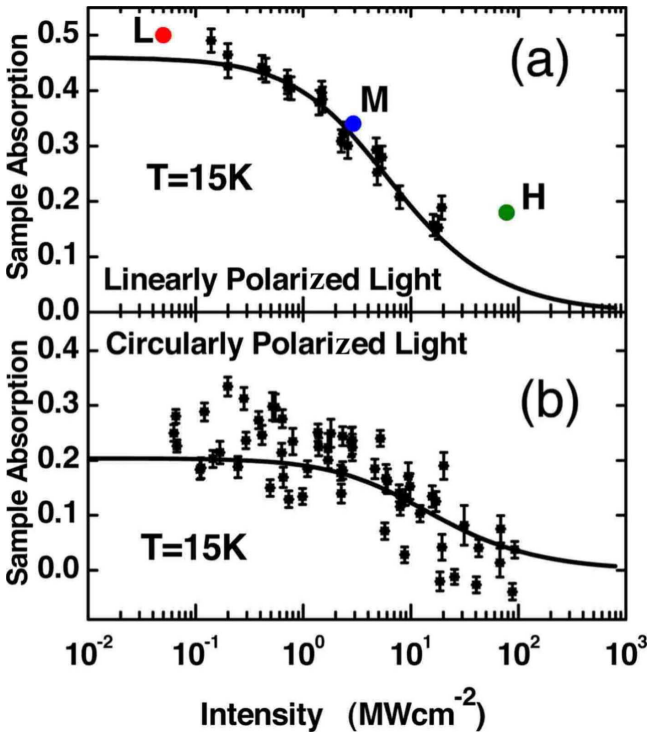

FIG. 4. (Color online) (a) Sample saturation characteristic using linearly polarized light. The absolute sample absorption [calculated as $\ln(T_s/T_p)$] is plotted against the light intensity inside the sample, corrected for the geometrical effects detailed in the text. (b) The lower plot presents data from saturating the sample with circularly polarized light [absorption$=-\ln(T_{\mathrm{circ}})$]. Both curves show theoretical fits, these are explained in the text. The points labeled L, M, and H correspond to the intensities of the polarization plots in Fig. 5.

Saturation experiments were performed by permuting a series of attenuators placed in front of and behind the bonded QW sample in a way that allowed the intensity at the sample to be varied over ~3 decades while keeping the variation at the detector to less than a factor of 3 and the net intensity well within the detector's linear-response range.[10] The saturation curves were measured with linearly polarized and then circularly polarized pulses in turn, in the same experimental run, so that the absolute intensity values could be compared with maximum confidence. Light from the laser was linearly polarized and an angle-tunable quarter-wave plate was used to convert this into circularly polarized light. Experiments were done with the sample cooled to 15 K, which maximized the sample's peak absorption, allowing the largest portion of the saturation characteristic to be accessed experimentally.

IV. RESULTS

Figure 4 compares the saturation curves for linearly and circularly polarized light. The scatter in the circularly polarized data set is larger because, with the equipment in the circularly polarized configuration, it proved impracticable to ratio out the effects of slight random beam misalignments (as

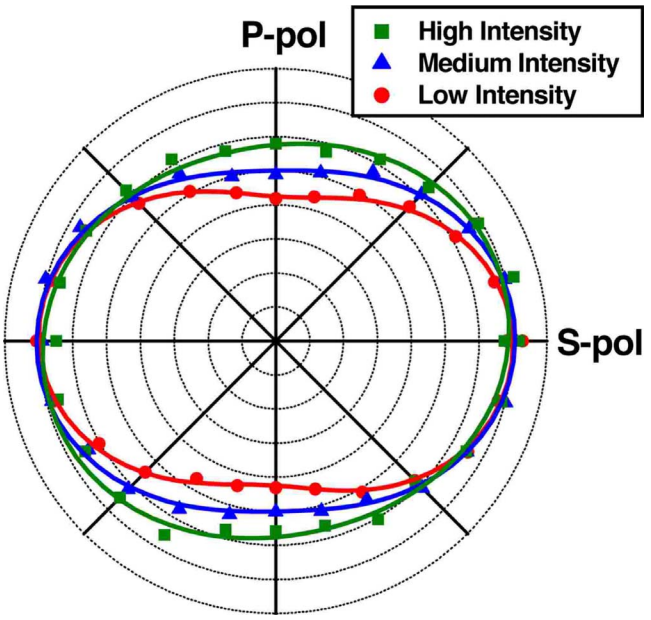

FIG. 5. (Color online) The polarizations of light leaving the sample were measured by rotating a linear polarizer and these plots show the resulting transmission for each angle. The incident light was circularly polarized and it can be seen that only light polarized along the sample's growth direction was absorbed. It can also be seen that the transition is saturating with the increasing intensities of incident light; this data is also shown Fig. 4.

the attenuators were moved around) by taking reference *s*-polarized spectra. However, a calibrated small-signal linear absorption spectrum of the sample was separately measured using weak circularly polarized light which was rationed with *s*-polarized spectrum and yielded a calibrated ISBT absorbance of $\alpha=-\ln(T_{\mathrm{circ}})=0.18(5)$, which was used to scale the saturation curve accordingly.

A glance at Fig. 4 is enough to show that although the small-signal circularly polarized sample absorption is half the linearly polarized value, the saturation intensity parameters have nothing like the disparity expected on the basis of the analysis in Sec. II B. Fitting the linearly polarized data as detailed in Sec. II A gives a saturation intensity of 1.8 ± 0.5 MW cm^{-2} and a low intensity sample absorption of 0.46(3) which combine to give an estimate of the relaxation time of $\tau_{21}\sim1.3(4)$ ps. However, applying the same analytical process to the circularly polarized data (not shown) gives $\alpha=0.3(1)$ and $I_{\mathrm{sat}}=3\pm2$ MW cm^{-2}. Rather than being 10–80 times smaller, the circularly polarized I_{sat} values are coming out approximately twice as large as the linearly polarized case.

To investigate why this occurred, the polarization state of the light transmitted by the sample was mapped out in detail (Fig. 5). The results are consistent with the conventional classical picture of a saturable linearly polarized dipole that absorbs only light polarized parallel to the growth direction, and additionally, it is only this component of the absorption is saturating. The three different intensities used to plot Fig. 5 span the whole of the saturation curve in Fig. 4(a). They are fully consistent with the rest of the saturation data and clearly imply that a naive application of the spin-pumping model of Sec. II B is inappropriate to this situation.

If we ignore the quantum nature of the electronic spin system completely and instead work within the semiclassical picture, the circularly polarized saturation curve would be expected to be a simple transformation of the linearly polarized case. Allowing for the fact that, in effect, only half the intensity of the circularly polarized beam can couple to the *p*-polarized ISBT, we would expect a sample absorption given by

$$\alpha_{\mathrm{circ}}=\ln\left\{\frac{2}{1+\exp[-\alpha_{12}(I/2)]}\right\}, \tag{15}$$

where the sample's absorption was calculated as being $-\ln(\text{transmission})$ and $\alpha_{12}(I/2)$ is the sample absorption for light linearly *p*-polarized along the growth direction and with half of the intensity. Using this expression with the data from Fig. 4(b) generates the saturation characteristic curve of Fig. 4(a). The fit is acceptable, implying the data set can be fully described without invoking any spin-pumping or spin-dependent saturation effects.

V. DISCUSSION

Viewing the problem classically, our QW absorption saturation results can be understood in terms of absorption by a plane of saturable dipole oscillators, each of which are perfectly polarized in the *z* direction. Absorption of obliquely incident circularly polarized light can be understood by resolving it into *s*- and *p*-polarized components and allowing only the latter to couple to the ISBT. The problem with this simple picture though is that it says nothing about how the effect on the sample differs between the case when it is partly absorbing a helical beam and when it is completely absorbing a linearly *p*-polarized one. In other words, this classical description tells us nothing about how the QWs absorb a helically polarized beam's angular momentum.

The electron states in the QWs can be modeled to the first order using the envelope function approximation; where the wave function is the product of a cell-periodic component (with *s* symmetry) and a comparatively slowly varying envelope function. The envelope function corresponds to perfect electron confinement in the *z* direction, contrasted with free, approximately translationally invariant and two-dimensionally isotropic, electron motion in the other two. Although the spin-relaxation mechanisms in these samples are still poorly understood, the *s* symmetry of the cell-periodic component of the wave function argues that the spin-relaxation times, τ_s, should not be highly sensitive to the orientation of the electron spin.

If we consider for the moment the case of a normally incident circularly polarized light field absorbed by an ISBT. The 2D isotropic nature of the electron motion implies that if the light is absorbed, its angular momentum can go only into the electron-spin system since the electron orbital system appears rotationally symmetric to such light field so there is no mechanism for the field to exert a torque on it. However, in the case of conduction-band ISBTs, such spin-flipping normal incidence absorption is well known to be extremely weak. It occurs at a level typically $<1\%$ (Ref. 18) of the

normal dipole-allowed ISBT mechanism and only in the presence of higher-order band-structure effects or applied magnetic fields.[2,18] Although background-free photovoltage measurements[2] can detect the spin polarization it produces, it plays a negligible role in these all-optical experiments, which are sensitive to the absorption by the whole electron population.

Returning to the case of obliquely incident light and viewing the problem quantum mechanically allows us to reexamine the issue of angular momentum conservation. Now the absorption is viewed as a series of annihilation events of photons each of which carry values of spin angular momentum vectors, $\pm\hbar$, aligned along the propagation direction of the beam. If the QW absorbs (say) a σ^+ photon traveling at 45° to the QW plane, the same symmetry-based arguments as those above argue that in the limit of perfect 2D confinement the absorption strength of the mechanism that couples to the z component of the photon's angular momentum vector is, to first order in the band structure, vanishingly small because it relates to field components oscillating in the QW plane.

Now, our saturation data, in this geometry, also argue that the xy component of the photons angular momentum vector is not coupling to the electron-spin system either. If it were, we would have expected to see the much lower saturation intensity characteristic predicted by Eq. (14).

In addition, since in the perfect 2D case the electrons are free to move only in the xy plane they are prevented from acquiring any z component of their motion which would be needed to give them a nonzero xy vector component of orbital angular momentum. This constraint prohibits the electron orbital system from taking up the xy component of the annihilated photon's angular momentum.

In conclusion, we argue that, both from the classical and quantum view points, these data are consistent with a situation where the angular momentum of a circularly polarized beam traveling with a velocity component along the QW planes couples neither to the spin nor to the orbital parts of the electron angular momentum system. It would appear that electric fields in such a helical beam act on the electrons; but since the electrons' wave function orientations are defined by the confining potentials of the 2D heterostructure, the forces are then transferred to act directly on the crystal lattice.

The result is that the angular momentum of the beam completely bypasses both the electron-spin and orbital angular momentum systems, and it instead exerts a torque on the crystal as a whole.

ACKNOWLEDGMENT

The support of the U.K. Engineering and Physical Sciences Research Council is gratefully acknowledged.

[1] I. Žutić, J. Fabian, and S. Das Sarma, Rev. Mod. Phys. **76**, 323 (2004).
[2] S. D. Ganichev, P. Schneider, V. V. Belkov, E. L. Ivchenko, S. A. Tarasenko, W. Wegscheider, D. Weiss, D. Schuh, B. N. Murdin, P. J. Phillips, C. R. Pidgeon, D. G. Clarke, M. Merrick, P. Murzyn, E. V. Beregulin, and W. Prettl, Phys. Rev. B **68**, 081302(R) (2003).
[3] S. D. Ganichev and W. Prett, J. Phys.: Condens. Matter **15**, R935 (2003).
[4] J. B. Khurgin, Appl. Phys. Lett. **88**, 123511 (2006).
[5] S. D. Ganichev, S. N. Danilov, V. V. Bel'kov, E. L. Ivchenko, M. Bichler, W. Wegscheider, D. Weiss, and W. Prettl, Phys. Rev. Lett. **88**, 057401 (2002).
[6] M. Helm, in *Intersubband Transitions in Quantum Wells: Physics and Device Applications I*, Semiconductors and Semimetals Vol. 62, edited by H. C. Liu and F. Capasso (Academic, New York, 2000), Chap. 1.
[7] B. F. Levine, J. Appl. Phys. **74**, R1 (1993).
[8] R. Loudon, *The Quantum Theory of Light*, 3rd ed. (Oxford University Press, Oxford, 2000).
[9] J. F. Dynes, M. D. Frogley, M. Beck, J. Faist, and C. C. Phillips, Phys. Rev. Lett. **94**, 157403 (2005).
[10] R. J. Steed, Ph.D. thesis, University of London, 2008.
[11] S. Nemoto, Appl. Opt. **27**, 1833 (1988).
[12] B. Noble and J. W. Daniel, *Applied Linear Algebra*, 3rd ed. (Prentice-Hall, Englewood Cliffs, NJ, 1987).
[13] Y. Ohno, R. Terauchi, T. Adachi, F. Matsukura, and H. Ohno, Physica E (Amsterdam) **6**, 817 (2000).
[14] A. Malinowski, R. S Britton, T. Grevatt, R. T. Harley, D. A. Ritchie, and M. Y. Simmons, Phys. Rev. B **62**, 13034 (2000).
[15] K. L. Vodopyanov, V. Chazapis, C. C. Phillips, B. Sung, and J. S. Harris, Jr., Semicond. Sci. Technol. **12**, 708 (1997).
[16] K. L. Vodopyanov, J. Opt. Soc. Am. B **16**, 1579 (1999).
[17] K. L. Vodopyanov and V. Chazapis, Opt. Commun. **135**, 98 (1997).
[18] S. A. Tarasenko, E. L. Ivchenko, V. V. Bel'kov, S. D. Ganichev, D. Schowalter, P. Schneider, M. Sollinger, W. Prettl, V. M. Ustinov, A. E. Zhukov, and L. E. Vorobjev, J. Supercond. **16**, 419 (2003).